



ALMA MATER STUDIORUM
UNIVERSITÀ DI BOLOGNA

ARCHIVIO ISTITUZIONALE
DELLA RICERCA

Alma Mater Studiorum Università di Bologna
Archivio istituzionale della ricerca

Hygro-thermal vibrations and buckling of laminated nanoplates via nonlocal strain gradient theory

This is the final peer-reviewed author's accepted manuscript (postprint) of the following publication:

Published Version:

Tocci Monaco G., Fantuzzi N., Fabbrocino F., Luciano R. (2021). Hygro-thermal vibrations and buckling of laminated nanoplates via nonlocal strain gradient theory. COMPOSITE STRUCTURES, 262, 1-10 [10.1016/j.compstruct.2020.113337].

Availability:

This version is available at: <https://hdl.handle.net/11585/809903> since: 2024-09-19

Published:

DOI: <http://doi.org/10.1016/j.compstruct.2020.113337>

Terms of use:

Some rights reserved. The terms and conditions for the reuse of this version of the manuscript are specified in the publishing policy. For all terms of use and more information see the publisher's website.

This item was downloaded from IRIS Università di Bologna (<https://cris.unibo.it/>).
When citing, please refer to the published version.

(Article begins on next page)

Hygro-Thermal Vibrations and Buckling of laminated nanoplates via Nonlocal Strain Gradient Theory

Giovanni Tocci Monaco^{1,2}, Nicholas Fantuzzi^{1,*}, Francesco Fabbrocino³,
Raimondo Luciano²

Abstract

Vibrations and buckling of thin laminated composite nano plates in hygrothermal environment are investigated using second-order strain gradient theory. Hamilton's principle is used in order to carry out motion equations. To obtain analytical solution Navier displacement field has been considered for both cross- and angle-ply laminates. Numerical solutions are provided and discussed in terms of plate aspect ratio and non local ratio for a large number of laminates. Whenever possible a comparison with classical analytical solutions is reported for buckling loads and fundamental frequencies. This work shows a large variety of angle-ply cases which are not common in the published literature. Moreover, critical temperatures for cross- and angle-ply laminates are shown for buckling and free vibration analyses.

Keywords: Kirchhoff plate's theory, Non-local theory, Strain gradient theory, Hygrothermal load, Buckling, Free vibration, Composite nanoplates, Cross- and Angle-ply laminates

1. Introduction

In the last decades MEMS (Micro-Electro-Mechanical-System) and NEMS (Nano-Electro-Mechanical-System) have become topics of great interest because of their large number of applications in many industrial fields [1, 2, 3, 4]. These kind of structures, such as nanoplates, nanorods, nanobeams, can be

*Corresponding email: nicholas.fantuzzi@unibo.it

¹DICAM Department University of Bologna, Italy

²Engineering Department, Parthenope University, Italy

³Department of Engineering, Telematic University Pegaso, Italy

6 used in medicine [5], electronics [6], aerospace [7] and even in civil construc-
7 tion [8]. To properly describe the behaviour of nanostructures it is necessary
8 to use theories that take into account the nano size effect, like long range
9 atomic interaction [9, 10]. Effects at the nano scale have been experimentally
10 measured in [11, 12]. Non-local theories have been widely used for the study
11 of nanostructures since Eringen developed his theory of non-local elasticity
12 [13]. These theories consider the nano scale effects thanks to the introduction
13 of one or more length scale parameters in addition to well know linear elastic
14 Lamé parameters [14, 15, 16, 17]. The classification of nonlocal theories is
15 generally presented as: strain gradient [18, 19, 20, 21], stress gradient [22],
16 modified strain gradient [23, 24, 25], couple stress [26], modified couple stress
17 [27, 28], integral type [29, 30] and micropolar [31, 32, 33]. In [34] strain and
18 stress gradient non local theory is used to study dynamic and buckling prob-
19 lems of elastic nanobeams. Nanoplates subjected to hygrothermal loads were
20 also investigated in the works [35, 36, 37, 38], using different non-local theo-
21 ries. In [39, 40] the influence of the non-local parameter on the critical load is
22 studied and the solution for the problem of buckling of ccomposite nanoplates
23 is provided. In [41] different non-local theories were employed to model the
24 vibrational behavior of plates. Civalek et al. [42] presented numerical stud-
25 ies for dimensionless natural frequencies of different truss and frame models,
26 investigating the influences of the nonlocal parameter. In [43], thermally
27 induced dynamic behaviors of functionally graded flexoelectric nanobeams
28 (FGFNs) are analyzed using simplified strain gradient nonlocal theory. The
29 effect of thermal, hygrometric and piezoelectric stress on composite plates
30 and shells has been investigated by [44, 45, 46, 47].

31 The focus of this paper is the study of buckling and free vibrations of lam-
32 inated composite nano plates in hygrothermal environment. In particular,
33 for the buckling analysis it will look for the temperature value and the combi-
34 nation of temperature and humidity that leads to the instability of the plate,
35 while for the dynamic case it will investigate the influence that the thermal
36 load has on the natural vibration frequencies. This paper is structured as de-
37 scribed below. After the introduction section, the theoretical background for
38 laminated thin plates in hygrothermal environment is developed introducing
39 also the non-linear terms of von Karman that allow to perform the linear
40 analysis of buckling. Using second order strain gradient theory non local
41 effect are take into account. The analytical solution is obtained using Navier
42 developments in double trigonometric series. Then, in order to validate the
43 calculation code, implemented in MATLAB, various comparisons with the

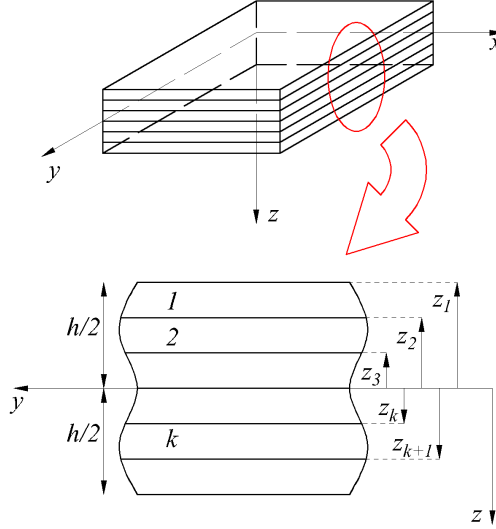


Figure 1: Laminate general layout.

44 literature are reported [48, 49, 50, 51]. After the comparisons, the results
 45 for buckling and free vibration obtained for different lamination schemes and
 46 different types of load are provided. Finally, a conclusion section is reported
 47 at the end of this paper.

48 2. Theoretical background

49 Consider a laminated thin nanoplate, modeled with the Kirchhoff plate
 50 assumptions modified to take into account the non linear terms of von Kar-
 51 man, subjected to hygrothermal stresses. The plate is composed of k or-
 52 thotropic layers oriented at angles $\theta^{(1)}, \theta^{(2)}, \dots, \theta^{(k)}$. The thickness of the
 53 k -th oriented layer, along the z axis, is defined as $h_k = z_{k+1} - z_k$. Introduced
 54 the reference system as in figure 1, we can define the displacement field of a
 55 generic point of the solid by means of the triad of displacement components
 56 U, V, W , which are functions of the coordinates (x, y, z) .

$$\begin{aligned}
 U(x, y, z, t) &= u(x, y, t) - z \frac{\partial w}{\partial x} \\
 V(x, y, z, t) &= v(x, y, t) - z \frac{\partial w}{\partial y} \\
 W(x, y, z, t) &= w(x, y, t)
 \end{aligned} \tag{1}$$

57 where u, v and w are the displacements along the x, y and z axis of the
 58 point on the middle surface and $\partial w/\partial x$ and $\partial w/\partial y$ are the corresponding
 59 rotations. The plate strains are defined as:

$$\boldsymbol{\varepsilon} = \boldsymbol{\varepsilon}^{(0)} + z\boldsymbol{\varepsilon}^{(1)} \quad (2)$$

60 where

$$\boldsymbol{\varepsilon}^{(0)} = \begin{Bmatrix} \varepsilon_{xx}^{(0)} \\ \varepsilon_{yy}^{(0)} \\ \gamma_{xy}^{(0)} \end{Bmatrix} = \begin{Bmatrix} \frac{\partial u}{\partial x} + \frac{1}{2} \left(\frac{\partial w}{\partial x} \right)^2 \\ \frac{\partial v}{\partial y} + \frac{1}{2} \left(\frac{\partial w}{\partial y} \right)^2 \\ \frac{\partial u}{\partial y} + \frac{\partial v}{\partial x} + \frac{\partial w}{\partial x} \frac{\partial w}{\partial y} \end{Bmatrix}, \quad \boldsymbol{\varepsilon}^{(1)} = \begin{Bmatrix} \varepsilon_{xx}^{(1)} \\ \varepsilon_{yy}^{(1)} \\ \gamma_{xy}^{(1)} \end{Bmatrix} = \begin{Bmatrix} -\frac{\partial^2 w}{\partial x^2} \\ -\frac{\partial^2 w}{\partial y^2} \\ -2\frac{\partial^2 w}{\partial x \partial y} \end{Bmatrix} \quad (3)$$

61 In order to take into account non local effects, the second order strain gradient
 62 theory is introduced as follows

$$\begin{aligned} \begin{Bmatrix} \sigma_{xx} \\ \sigma_{yy} \\ \sigma_{xy} \end{Bmatrix}^{(k)} &= (1 - \ell^2 \nabla^2) \begin{bmatrix} \bar{Q}_{11} & \bar{Q}_{12} & \bar{Q}_{16} \\ \bar{Q}_{12} & \bar{Q}_{22} & \bar{Q}_{26} \\ \bar{Q}_{16} & \bar{Q}_{26} & \bar{Q}_{66} \end{bmatrix}^{(k)} \begin{Bmatrix} \varepsilon_{xx} \\ \varepsilon_{yy} \\ \gamma_{xy} \end{Bmatrix} \\ &- \begin{bmatrix} \bar{Q}_{11} & \bar{Q}_{12} & \bar{Q}_{16} \\ \bar{Q}_{12} & \bar{Q}_{22} & \bar{Q}_{26} \\ \bar{Q}_{16} & \bar{Q}_{26} & \bar{Q}_{66} \end{bmatrix}^{(k)} \begin{Bmatrix} \alpha_{xx} \Delta T + \beta_{xx} \Delta C \\ \alpha_{yy} \Delta T + \beta_{yy} \Delta C \\ 2\alpha_{xy} \Delta T + 2\beta_{xy} \Delta C \end{Bmatrix}^{(k)} \end{aligned} \quad (4)$$

63 where the subscript $^{(k)}$ indicates the k -th orthotropic lamina, ℓ is the nonlocal
 64 parameter and the operator $\nabla^2 = \partial^2/\partial x^2 + \partial^2/\partial y^2$.

65 A linear variation of hygrothermal loads along the thickness is assumed:

$$\begin{aligned} \Delta T &= T_0 + zT_1/h \\ \Delta C &= C_0 + zC_1/h \end{aligned} \quad (5)$$

66 It is underlined that the $\bar{Q}_{ij}^{(k)}$ represent the engineering constants ori-
 67 ented towards the reference system of the problem [48]. The hygrothermal
 68 properties of each ply have to be oriented also:

$$\begin{aligned} \boldsymbol{\alpha}^{(k)} &= \begin{Bmatrix} \alpha_{xx} \\ \alpha_{yy} \\ 2\alpha_{xy} \end{Bmatrix}^{(k)} = \begin{Bmatrix} \alpha_1^{(k)} \cos^2 \theta^{(k)} + \alpha_2^{(k)} \sin^2 \theta^{(k)} \\ \alpha_1^{(k)} \sin^2 \theta^{(k)} + \alpha_2^{(k)} \cos^2 \theta^{(k)} \\ 2 \left(\alpha_1^{(k)} - \alpha_2^{(k)} \right) \sin \theta^{(k)} \cos \theta^{(k)} \end{Bmatrix} \\ \boldsymbol{\beta}^{(k)} &= \begin{Bmatrix} \beta_{xx} \\ \beta_{yy} \\ 2\beta_{xy} \end{Bmatrix}^{(k)} = \begin{Bmatrix} \beta_1^{(k)} \cos^2 \theta^{(k)} + \beta_2^{(k)} \sin^2 \theta^{(k)} \\ \beta_1^{(k)} \sin^2 \theta^{(k)} + \beta_2^{(k)} \cos^2 \theta^{(k)} \\ 2 \left(\beta_1^{(k)} - \beta_2^{(k)} \right) \sin \theta^{(k)} \cos \theta^{(k)} \end{Bmatrix} \end{aligned} \quad (6)$$

69 By integrating the stresses along the thickness we obtain:

$$\begin{aligned}\mathbf{N} &= \begin{Bmatrix} N_{xx} \\ N_{yy} \\ N_{xy} \end{Bmatrix} = \sum_{k=1}^{N_L} \int_{z_k}^{z_{k+1}} \begin{Bmatrix} \sigma_{xx} \\ \sigma_{yy} \\ \sigma_{xy} \end{Bmatrix}^{(k)} dz \\ \mathbf{M} &= \begin{Bmatrix} M_{xx} \\ M_{yy} \\ M_{xy} \end{Bmatrix} = \sum_{k=1}^{N_L} \int_{z_k}^{z_{k+1}} \begin{Bmatrix} \sigma_{xx} \\ \sigma_{yy} \\ \sigma_{xy} \end{Bmatrix}^{(k)} z dz\end{aligned}\quad (7)$$

70 Such definition of stress resultants allows to define \mathbf{A}, \mathbf{D} and \mathbf{B} matrices,
71 called *membrane stiffness matrix*, *bending stiffness matrix* and *bending-membrane*
72 *coupling stiffness matrix* [48], and vectors $\mathbf{A}^\alpha, \mathbf{A}^\beta, \mathbf{B}^\alpha, \mathbf{B}^\beta, \mathbf{D}^\alpha$ and \mathbf{D}^β con-
73 taining the hygrothermal properties of the laminate

$$\begin{aligned}\mathbf{A}^\alpha &= \sum_{k=1}^{N_L} \int_{z_k}^{z_{k+1}} \bar{\mathbf{Q}}^{(k)} \boldsymbol{\alpha}^{(k)} dz = \sum_{k=1}^{N_L} \bar{\mathbf{Q}}^{(k)} \boldsymbol{\alpha}^{(k)} (z_{k+1} - z_k) \\ \mathbf{B}^\alpha &= \sum_{k=1}^{N_L} \int_{z_k}^{z_{k+1}} \bar{\mathbf{Q}}^{(k)} \boldsymbol{\alpha}^{(k)} z dz = \frac{1}{2} \sum_{k=1}^{N_L} \bar{\mathbf{Q}}^{(k)} \boldsymbol{\alpha}^{(k)} (z_{k+1}^2 - z_k^2) \\ \mathbf{D}^\alpha &= \sum_{k=1}^{N_L} \int_{z_k}^{z_{k+1}} \bar{\mathbf{Q}}^{(k)} \boldsymbol{\alpha}^{(k)} z^2 dz = \frac{1}{3} \sum_{k=1}^{N_L} \bar{\mathbf{Q}}^{(k)} \boldsymbol{\alpha}^{(k)} (z_{k+1}^3 - z_k^3)\end{aligned}\quad (8)$$

$$\begin{aligned}\mathbf{A}^\beta &= \sum_{k=1}^{N_L} \int_{z_k}^{z_{k+1}} \bar{\mathbf{Q}}^{(k)} \boldsymbol{\beta}^{(k)} dz = \sum_{k=1}^{N_L} \bar{\mathbf{Q}}^{(k)} \boldsymbol{\beta}^{(k)} (z_{k+1} - z_k) \\ \mathbf{B}^\beta &= \sum_{k=1}^{N_L} \int_{z_k}^{z_{k+1}} \bar{\mathbf{Q}}^{(k)} \boldsymbol{\beta}^{(k)} z dz = \frac{1}{2} \sum_{k=1}^{N_L} \bar{\mathbf{Q}}^{(k)} \boldsymbol{\beta}^{(k)} (z_{k+1}^2 - z_k^2) \\ \mathbf{D}^\beta &= \sum_{k=1}^{N_L} \int_{z_k}^{z_{k+1}} \bar{\mathbf{Q}}^{(k)} \boldsymbol{\beta}^{(k)} z^2 dz = \frac{1}{3} \sum_{k=1}^{N_L} \bar{\mathbf{Q}}^{(k)} \boldsymbol{\beta}^{(k)} (z_{k+1}^3 - z_k^3)\end{aligned}\quad (9)$$

74

the stress characteristics take the following form:

$$\begin{aligned}
\begin{Bmatrix} N_{xx} \\ N_{yy} \\ N_{xy} \end{Bmatrix} &= (1 - \ell^2 \nabla^2) \left(\begin{bmatrix} A_{11} & A_{12} & A_{16} \\ A_{12} & A_{22} & A_{26} \\ A_{16} & A_{26} & A_{66} \end{bmatrix} \begin{Bmatrix} \varepsilon_{xx}^{(0)} \\ \varepsilon_{yy}^{(0)} \\ \gamma_{xy}^{(0)} \end{Bmatrix} + \begin{bmatrix} B_{11} & B_{12} & B_{16} \\ B_{12} & B_{22} & B_{26} \\ B_{16} & B_{26} & B_{66} \end{bmatrix} \begin{Bmatrix} \varepsilon_{xx}^{(1)} \\ \varepsilon_{yy}^{(1)} \\ \gamma_{xy}^{(1)} \end{Bmatrix} \right) \\
&\quad - \begin{Bmatrix} A_1^\alpha \\ A_2^\alpha \\ A_6^\alpha \end{Bmatrix} T_0 - \begin{Bmatrix} B_1^\alpha \\ B_2^\alpha \\ B_6^\alpha \end{Bmatrix} \frac{1}{h} T_1 - \begin{Bmatrix} A_1^\beta \\ A_2^\beta \\ A_6^\beta \end{Bmatrix} C_0 - \begin{Bmatrix} B_1^\beta \\ B_2^\beta \\ B_6^\beta \end{Bmatrix} \frac{1}{h} C_1
\end{aligned} \tag{10}$$

$$\begin{aligned}
\begin{Bmatrix} M_{xx} \\ M_{yy} \\ M_{xy} \end{Bmatrix} &= (1 - \ell^2 \nabla^2) \left(\begin{bmatrix} B_{11} & B_{12} & B_{16} \\ B_{12} & B_{22} & B_{26} \\ B_{16} & B_{26} & B_{66} \end{bmatrix} \begin{Bmatrix} \varepsilon_{xx}^{(0)} \\ \varepsilon_{yy}^{(0)} \\ \gamma_{xy}^{(0)} \end{Bmatrix} + \begin{bmatrix} D_{11} & D_{12} & D_{16} \\ D_{12} & D_{22} & D_{26} \\ D_{16} & D_{26} & D_{66} \end{bmatrix} \begin{Bmatrix} \varepsilon_{xx}^{(1)} \\ \varepsilon_{yy}^{(1)} \\ \gamma_{xy}^{(1)} \end{Bmatrix} \right) \\
&\quad - \begin{Bmatrix} B_1^\alpha \\ B_2^\alpha \\ B_6^\alpha \end{Bmatrix} T_0 - \begin{Bmatrix} D_1^\alpha \\ D_2^\alpha \\ D_6^\alpha \end{Bmatrix} \frac{1}{h} T_1 - \begin{Bmatrix} B_1^\beta \\ B_2^\beta \\ B_6^\beta \end{Bmatrix} C_0 - \begin{Bmatrix} D_1^\beta \\ D_2^\beta \\ D_6^\beta \end{Bmatrix} \frac{1}{h} C_1
\end{aligned} \tag{11}$$

75

76

In order to carry out the equations of motion the Hamilton's principle is employed

$$\int_0^T (\delta U + \delta V - \delta K) dt = 0 \tag{12}$$

77

78

where δU is the virtual strain energy, δV is the virtual work done by the applied forces and δK is the virtual kinetic energy. Developing the terms in

79 equation (12) the Hamilton's principle takes the following form:

$$\begin{aligned}
& \int_0^T \left[\int_{\mathcal{A}} \left[\begin{array}{c} \delta u_{,x} \\ \delta u_{,y} \\ \delta v_{,x} \\ \delta v_{,y} \\ \delta w_{,xx} \\ \delta w_{,yy} \\ \delta w_{,xy} \end{array} \right]^{\top} \begin{bmatrix} \mathcal{T}_{11} & \mathcal{T}_{12} & \mathcal{T}_{13} \\ \mathcal{T}_{21} & \mathcal{T}_{22} & \mathcal{T}_{23} \\ \mathcal{T}_{31} & \mathcal{T}_{32} & \mathcal{T}_{33} \\ \mathcal{T}_{41} & \mathcal{T}_{42} & \mathcal{T}_{43} \\ \mathcal{T}_{51} & \mathcal{T}_{52} & \mathcal{T}_{53} \\ \mathcal{T}_{61} & \mathcal{T}_{62} & \mathcal{T}_{63} \\ \mathcal{T}_{71} & \mathcal{T}_{72} & \mathcal{T}_{73} \end{bmatrix} \begin{Bmatrix} u \\ v \\ w \end{Bmatrix} - \{ \delta w_{,x} \quad \delta w_{,y} \} \begin{bmatrix} \hat{N}_{xx} & \hat{N}_{xy} \\ \hat{N}_{xy} & \hat{N}_{yy} \end{bmatrix} \begin{Bmatrix} w_{,x} \\ w_{,y} \end{Bmatrix} \right. \\
& \left. \begin{array}{c} \left(\begin{array}{c} \delta \ddot{u} \\ \delta \ddot{v} \\ \delta \ddot{w} \\ \delta \ddot{w}_{,x} \\ \delta \ddot{w}_{,y} \end{array} \right)^{\top} \begin{bmatrix} I_0 & 0 & 0 & -I_1 & 0 \\ 0 & I_0 & 0 & 0 & -I_1 \\ 0 & 0 & I_0 & 0 & 0 \\ -I_1 & 0 & 0 & I_2 & 0 \\ 0 & -I_1 & 0 & 0 & I_2 \end{bmatrix} \begin{Bmatrix} \delta u \\ \delta v \\ \delta w \\ \delta w_{,x} \\ \delta w_{,y} \end{Bmatrix} \right] dx dy \Big] dt \\
& + \text{boundary integral terms} = 0
\end{aligned} \tag{13}$$

80 where the variational form of the displacement field is identified by δ , while
81 its corresponding derivatives in time by the dots, the terms \mathcal{T}_{ij} are shown
82 in [52], \hat{N}_{xx} , \hat{N}_{yy} and \hat{N}_{xy} (defined in eq. (10)) identify the axial and shear
83 buckling terms, including hygrothermal terms, and I_0, I_1 and I_2 are the mass
84 inertias which can be defined as it follows:

$$I_i = \rho \sum_{k=1}^{N_L} \int_{z_k}^{z_{k+1}} z^i dz \tag{14}$$

85 where $i = 0, 1, 2$.

86 3. Navier solution

87 The Navier solution is obtained for cross- and angle-ply laminates. This
88 kind of solution allows to solve the case of simply supported plates [48].

89 For cross-ply laminates it is needed that $A_{16} = A_{26} = B_{16} = B_{26} = D_{16} =$

90 $D_{26} = 0$, and the displacement field it is assumed to be:

$$\begin{aligned}
u(x, y) &= \sum_{m=1}^{\infty} \sum_{n=1}^{\infty} U_{mn} \cos \alpha x \sin \beta y \\
v(x, y) &= \sum_{m=1}^{\infty} \sum_{n=1}^{\infty} V_{mn} \sin \alpha x \cos \beta y \\
w(x, y) &= \sum_{m=1}^{\infty} \sum_{n=1}^{\infty} W_{mn} \sin \alpha x \sin \beta y
\end{aligned} \tag{15}$$

91 For angle-ply laminates it is needed that $A_{16} = A_{26} = B_{11} = B_{12} = B_{22} =$
92 $B_{66} = D_{16} = D_{26} = 0$, and the displacement field it is assumed to be:

$$\begin{aligned}
u(x, y) &= \sum_{m=1}^{\infty} \sum_{n=1}^{\infty} U_{mn} \sin \alpha x \cos \beta y \\
v(x, y) &= \sum_{m=1}^{\infty} \sum_{n=1}^{\infty} V_{mn} \cos \alpha x \sin \beta y \\
w(x, y) &= \sum_{m=1}^{\infty} \sum_{n=1}^{\infty} W_{mn} \sin \alpha x \sin \beta y
\end{aligned} \tag{16}$$

93 It is remarked the cross- and angle-ply laminated consider different kind of
94 simply-supported boundary conditions [48].

95 As described in [48] shear in-plane mechanical load $\hat{N}_{xy} = 0$ should be
96 neglected to solve the problem with Navier method. Since hygrothermal
97 loads consider all the in-plane loads coupled, contrary to the mechanical in-
98 plane loads, it is necessary that the lamination scheme for angle-ply plates
99 is anti-symmetric so that it gives $\hat{N}_{xy} = 0$ (see eq. (10)). All cross-ply
100 configurations have always $\hat{N}_{xy} = 0$.

101 3.1. Buckling

102 In this paragraph, the behavior of the plates subjected to thermal loads
103 that lead to the instability will be analyzed. The solution system is:

$$\begin{bmatrix} \hat{c}_{11} & \hat{c}_{12} & \hat{c}_{13} \\ \hat{c}_{12} & \hat{c}_{22} & \hat{c}_{23} \\ \hat{c}_{13} & \hat{c}_{23} & \hat{c}_{33} + \hat{t}_{buck} \end{bmatrix} \begin{Bmatrix} U_{mn} \\ V_{mn} \\ W_{mn} \end{Bmatrix} = \begin{Bmatrix} 0 \\ 0 \\ 0 \end{Bmatrix} \tag{17}$$

104 where the coefficients \hat{c}_{ij} are those shown in [52] for the cross- and angle-ply
 105 plates, and the term \tilde{t}_{buck} includes hygrothermal loads

$$\begin{aligned} \tilde{t}_{buck} = \bar{T} & \left(\alpha^2 \left(A_1^\alpha + \kappa_{c_0} A_1^\beta + \frac{\kappa_t}{h} B_1^\alpha + \frac{\kappa_{c_1}}{h} B_1^\beta \right) \right. \\ & \left. + \beta^2 \left(A_2^\alpha + \kappa_{c_0} A_2^\beta + \frac{\kappa_t}{h} B_2^\alpha + \frac{\kappa_{c_1}}{h} B_2^\beta \right) \right) \end{aligned} \quad (18)$$

106 where $\kappa_{c_0} = C_0/T_0$, $\kappa_t = T_1/T_0$ and $\kappa_{c_1} = C_1/T_0$.

107 From this last relation it can be deduced that the instability analysis can-
 108 not be performed with the load acting in one direction only because the type
 109 of load in question cannot be decoupled in two directions. As for the critical
 110 load, the critical temperature will be the lowest among the temperatures that
 111 lead to the instability of the plate.

$$T_{cr} = \min_{1 \leq m, n \leq \infty} \{ \bar{T}(m, n) \} \quad (19)$$

112 3.2. Free vibration

113 Replacing the Navier displacement field in the equations of motion and
 114 neglecting the rotary inertia, in the dynamic case, we obtain the following
 115 eigenvalue problem;

$$\left(\begin{bmatrix} \hat{c}_{11} & \hat{c}_{12} & \hat{c}_{13} \\ \hat{c}_{12} & \hat{c}_{22} & \hat{c}_{23} \\ \hat{c}_{13} & \hat{c}_{23} & \hat{c}_{33} + \tilde{t}_{buck} \end{bmatrix} - \omega^2 \begin{bmatrix} \hat{m}_{11} & 0 & 0 \\ 0 & \hat{m}_{22} & 0 \\ 0 & 0 & \hat{m}_{33} \end{bmatrix} \right) \begin{Bmatrix} U_{mn} \\ V_{mn} \\ W_{mn} \end{Bmatrix} = \begin{Bmatrix} 0 \\ 0 \\ 0 \end{Bmatrix} \quad (20)$$

116 where:

$$\begin{aligned} \hat{m}_{11} &= \hat{m}_{22} = I_0 \\ \hat{m}_{33} &= I_0 + I_2 (\alpha^2 + \beta^2) \end{aligned} \quad (21)$$

117 For a nontrivial solution the determinant of the coefficient matrix should be
 118 zero, which yields to the characteristic polynomial. The real positive roots
 119 of this cubic equation give the square of the natural frequency associated
 120 with mode (m, n) . The smallest of the frequencies is called the fundamental
 121 frequency. In the present case, the applied hygrothermal pre-stress influences
 122 the stiffness of the structure, thus, natural frequencies are obtained as a
 123 function of the pre-stress. There exist a value of the applied pre-stress that
 124 leads to null natural frequencies, such temperature values are defined as
 125 critical temperatures.

126 **4. Results and discussion**

127 In this section critical temperatures for the buckling and free vibration
 128 problems are discussed. Results are compared with the existing literature to
 129 validate the present model and novel applications are reported in order to
 130 demonstrate the influence of nanoscale parameter on the buckling and free
 131 vibration modes.

132 *4.1. Buckling*

133 The results of the first comparison are listed in table 1 with respect to the
 134 work [50], for a thin structure made of a single isotropic layer and a single
 135 orthotropic layer. For the isotropic configuration it has been considered:
 136 $E = 10^6$, $\nu = 0.3$, $\alpha_1/\alpha_0 = 1$, $\alpha_2/\alpha_0 = 1$, whereas for the orthotropic one:
 137 $E_1 = 15$, $E_2 = E_3 = 1$, $\nu_{12} = 0.3$, $\nu_{13} = 0.49$, $\nu_{23} = 0.3$, $G_{12} = 0.5$, $G_{13} =$
 138 0.3356 , $\alpha_1/\alpha_0 = 0.015$, $\alpha_2/\alpha_0 = 1$ where the normalization factor $\alpha_0 = 10^{-6}$
 139 is taken into consideration. The results are presented in dimensionless form
 140 according to the formula $\alpha_0 T_{cr} \cdot 10^3$, where T_{cr} is the critical temperature
 141 that leads the buckling into buckling mode.

Lamina	a/h	Ref. [50]	Present
Isotropic	100	0.1265	0.1265
Orthotropic	100	0.7480	0.7486

Table 1: $\alpha_0 T_{cr} \cdot 10^3$ of a single square isotropic layer and a single square orthotropic layer compared with the literature ($m, n = 1$).

142 Using the properties of the orthotropic layer of the first comparison lam-
 143 inates composed of multiple layers are analyzed. Results are shown in table
 144 2. It is noted that the symmetric configuration (0/90/0) buckles with a non
 145 symmetric number of waves one along x and two along y ($m = 1$ and $n = 2$),
 146 on the contrary the antisymmetric scheme (0/90) has a symmetric buckling
 147 mode ($m = n = 1$). In both cases very good agreement is shown with the
 148 present implementation.

149 Another comparison has been performed with respect to the work by Shi
 150 et al [51] and comparison is listed in table 3. Mechanical properties of the
 151 plate considered are $a = 38.1$ cm, $b = 30.5$ cm, $h = 0.12$ cm, $E_1 = 155$
 152 GPa, $E_2 = 8.07$ GPa, $G_{12} = 4.55$ GPa, $\nu_{12} = 0.22$, $\alpha_1 = -0.07 \cdot 10^{-6}$
 153 $^{\circ}\text{C}^{-1}$, $\alpha_2 = 30.1 \cdot 10^{-6} \text{ }^{\circ}\text{C}^{-1}$. Very good agreement is shown considering that
 154 laboratory experiments have been carried out in [51].

Layout	a/h	Ref. [50]	Present
$(0/90)^a$	100	0.4860	0.4863
$(0/90/0)^b$	100	0.9960	0.9944

Table 2: $\alpha_0 T_{cr} \cdot 10^3$ of a square nano-plates compared with the literature ^a $(m, n = 1)$, ^b $(m = 1, n = 2)$.

Layout	a/h	Ref. [51]	Present
$(0/90/90/0)_s$	317.5	6.8 °C	6.575 °C

Table 3: T_{cr} of a cross-ply nanoplate compared with the literature $(m, n) = 1$.

155 *4.1.1. In-plane thermal load*

156 For the analysis of laminates with different values of the non-local pa-
 157 rameter (tables 4, 5) the material properties are given as: $E_1/E_2 = var.$,
 158 $\nu_{12} = 0.25$, $\nu_{13} = \nu_{23} = 0$, $G_{12} = G_{13} = 0.5E_2$, $G_{23} = 0.2E_2$, $\alpha_1/\alpha_0 = 0.015$,
 159 $\alpha_2/\alpha_0 = 1$, $\beta_1 = 0$, $\beta_2 = 0.44$, where the stiffness ratio E_1/E_2 is variable and
 160 represents orthotropic material variation for a unitary in-plane transverse
 161 stiffness E_2 .

162 Please note that the units are not reported because a consistent system
 163 has been implicitly considered. moreover, with the present selection the
 164 results are dimensionless for the thermal case only. Whereas, the results will
 165 be reported in factorized form for the hygrothermal applications. The plates
 166 considered are rectangular with a ratio $a/h = 100$ and the total height of
 167 the laminate is kept constant independently on the number of plies in each
 168 stack.

169 From tables 4, 5 it can be noticed that the critical temperature is higher
 170 for angle-ply laminates than for cross-ply ones with the same number of lam-
 171 inae. For antisymmetric cross- and angle-ply plates the instability always
 172 occurs for $(m, n) = (1, 1)$, whereas for symmetrical cross-ply plates the in-
 173 stability comes for different values of (m, n) . In addition when the nonlocal
 174 parameter increases the critical temperature also increases.

175 Figure 2 displays different behaviours of cross- and angle-ply laminates
 176 by varying the geometric a/b and stiffness E_1/E_2 ratios for different values
 177 of the nonlocal parameter. It must be underlined that is considered $a = 1$ for
 178 the variation a/b , since such results are not reported in dimensionless form
 179 but they are factorized by $\alpha_0 T_{cr}$. The critical buckling temperatures increase
 180 almost exponentially by enlarging the plate width in the direction transverse

$(\ell/a)^2$	a/b	E_1/E_2				
		5	10	20	25	40
		(0/90/0)				
0.00	0.5	0.5246 ^(1,2)	0.7522 ^(1,3)	1.0529 ^(1,3)	1.1855 ^(1,3)	1.5277 ^(1,3)
	1.0	0.5246	0.7902	1.1309 ^(1,2)	1.2413 ^(1,2)	1.5302 ^(1,2)
	1.5	0.5803	0.7522	1.0529	1.1855	1.5277
0.05	0.5	0.9885	1.5702 ^(1,2)	2.4710 ^(1,2)	2.8591 ^(1,2)	3.8346 ^(1,2)
	1.0	1.0423	1.5702	2.4710	3.4050	3.8346
	1.5	1.5111	1.9587	2.7415	2.8591	3.9779
0.10	0.5	1.3656	2.3501 ^(1,2)	3.6984 ^(1,2)	4.2792 ^(1,2)	5.7392 ^(1,2)
	1.0	1.5601	2.3501	3.6984	4.2792	5.7392
	1.5	2.4418	3.1651	4.4301	4.9882	6.4280
		(0/90) ₂				
0.00	0.5	0.3494	0.5357	0.8510	0.9864	1.3267
	1.0	0.4908	0.7549	1.0688	1.2250	1.6174
	1.5	0.8432	1.2477	1.9323	2.2265	2.9657
0.05	0.5	0.5651	0.8663	1.3759	1.5949	2.1450
	1.0	0.9752	1.4018	2.1238	2.4341	3.2137
	1.5	2.1956	3.2489	5.0314	5.7975	7.7221
0.10	0.5	0.7807	1.1968	1.9008	2.2033	2.9634
	1.0	1.4597	2.0981	3.1787	3.6432	4.8101
	1.5	3.5480	5.2501	8.1304	9.3684	12.4785

Table 4: $\alpha_0 T_{cr} \cdot 10^3$ of different cross-ply laminates for different values of the geometric a/b and stiffness E_1/E_2 and the non-local parameter $(\ell/a)^2$. The superscripts indicate the number of semi-waves for which the plate becomes unstable (m,n) , where $(m,n) = (1,1)$ is not indicated.

$(\ell/a)^2$	a/b	E_1/E_2				
		5	10	20	25	40
$(-45/45)$						
0.00	0.5	0.2855	0.3580	0.4656	0.5102	0.6206
	1.0	0.4951	0.6418	0.8583	0.9478	1.1693
	1.5	0.7790	0.9967	1.3189	1.4521	1.7822
0.05	0.5	0.4617	0.5789	0.7528	0.8249	1.0034
	1.0	0.9839	1.2753	1.7054	1.8832	2.3232
	1.5	2.0283	2.5952	3.4340	3.7811	4.6404
0.10	0.5	0.6378	0.7997	1.0401	1.1397	1.3862
	1.0	1.4726	1.9088	2.5525	2.8186	3.4773
	1.5	3.2776	4.1938	5.5549	6.1102	7.4987
$(-45/45)_2$						
0.00	0.5	0.3827	0.6096	0.9932	1.1581	1.5723
	1.0	0.6809	1.1271	1.8820	2.2063	3.0209
	1.5	1.0607	1.7302	2.8627	3.3493	4.5716
0.05	0.5	0.6188	0.9856	1.6059	1.8725	2.5421
	1.0	1.3529	2.2397	3.7395	4.3839	6.0025
	1.5	2.7617	4.5052	7.4539	8.7209	11.9035
0.10	0.5	0.8549	1.3616	2.2186	2.5869	3.5120
	1.0	2.0249	3.3522	5.5969	6.5614	8.9840
	1.5	4.4629	7.2801	12.0450	14.0925	19.2354

Table 5: $\alpha_0 T_{cr} \cdot 10^3$ of different angle-ply laminates for different values of the geometric a/b and stiffness E_1/E_2 and the non-local parameter $(\ell/a)^2$. $(m, n) = (1, 1)$.

$(\ell/a)^2$	κ_t	E_1/E_2				
		5	10	20	25	40
0.00	0	0.8432	1.2477	1.9323	2.2265	2.9657
	5	0.9613	1.3916	2.0782	2.3584	3.0260
	10	1.1177	1.5730	2.2479	2.5068	3.0889
0.05	0	2.1956	3.2489	5.0314	5.7975	7.7221
	5	2.5029	3.6235	5.4112	6.1408	7.8792
	10	2.9103	4.0958	5.8532	6.5272	8.0428
0.10	0	3.5840	5.2501	8.1304	9.3684	12.4785
	5	4.0446	5.8554	8.7443	9.9231	12.7324
	10	4.7029	6.6186	9.4584	10.5477	12.9968

Table 6: $\alpha_0 T_{0,cr} \cdot 10^3$ of a rectangular plate ($a/b = 1.5$) with lamination layout $(0/90)_2$ for different value of ratio $\kappa_t = T_{1,cr}/T_{0,cr}$ and non local parameter $(\ell/a)^2 \cdot (m, n) = (1, 1)$.

181 to the fibers (zero fiber angle corresponds to the x axis which is related to
182 plate width a).

183 4.1.2. In-plane and bending thermal loads

184 The effect of constant and linear thermal loads is investigated below. The
185 aim is to show the effect of a linear temperature field to the buckling of the
186 plate, this effect is considered with the coefficient $\kappa_t = T_{1,cr}/T_{0,cr}$. Table 6
187 shows the buckling when combined thermal load for cross-ply laminates is
188 considered. The plate is of rectangular shape $a/b = 1.5$ with $a = 1$ and anti-
189 symmetric cross-ply configuration. It is clear that the buckling temperature
190 increases as the linear temperature increases, this induces the plate to show
191 a stiffer behavior. Such increase is observed by increasing the stiffness ratio
192 E_1/E_2 and the nonlocal parameter. Figure 3 shows the different behavior
193 of nanoplates when they are subjected to a uniform and linear combination
194 of temperature along the thickness for different geometric ratios a/b with
195 $a = 1$. It should be remarked that the effect of combining constant and
196 linear temperature distributions does not effect the critical temperature for
197 square plates since all the curves coincide for $a/b = 1$. Overall small effects
198 on the critical temperature are observed by including a linear temperature
199 distribution.

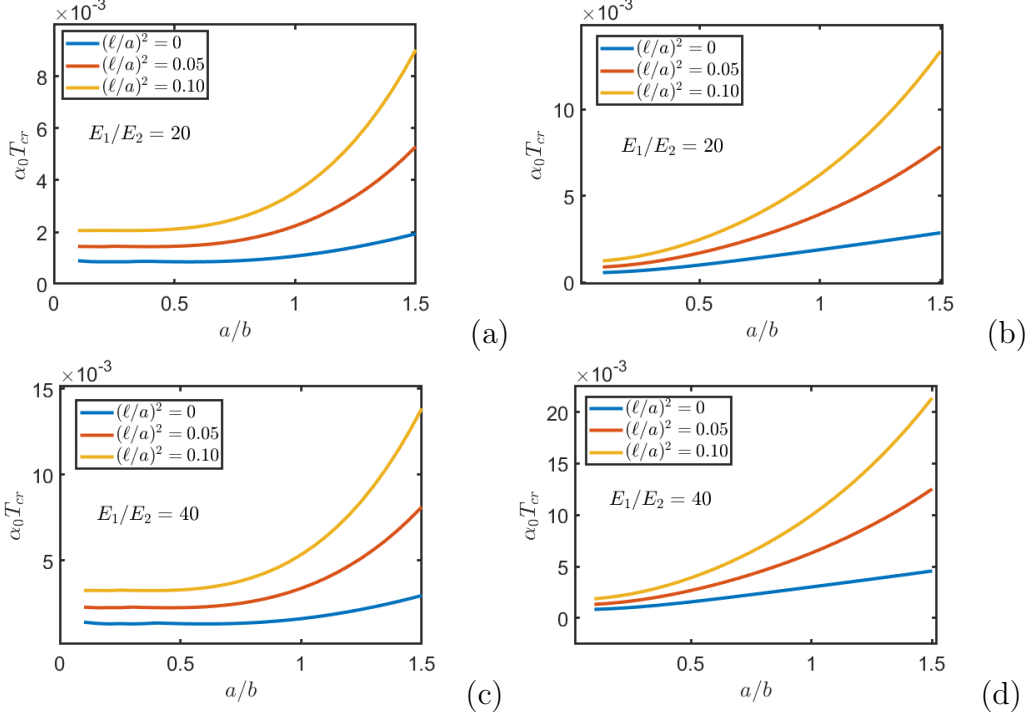


Figure 2: Critical temperature ($\alpha_0 T_{cr}$) of plates $(0/90)_2$ (a,c) and $(-45/45)_2$ (b,d) for different a/b and different value of non local parameter $(\ell/a)^2$.

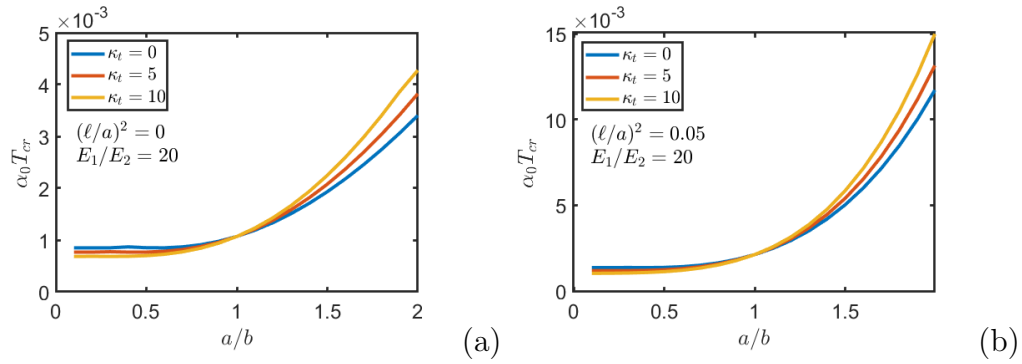


Figure 3: Critical temperature $\alpha_0 T_{cr}$ of plate with lamination layout $(0/90)_2$ for $(\ell/a)^2 = 0$ (a) and for $(\ell/a)^2 = 0.05$ (b) to vary of κ_t .

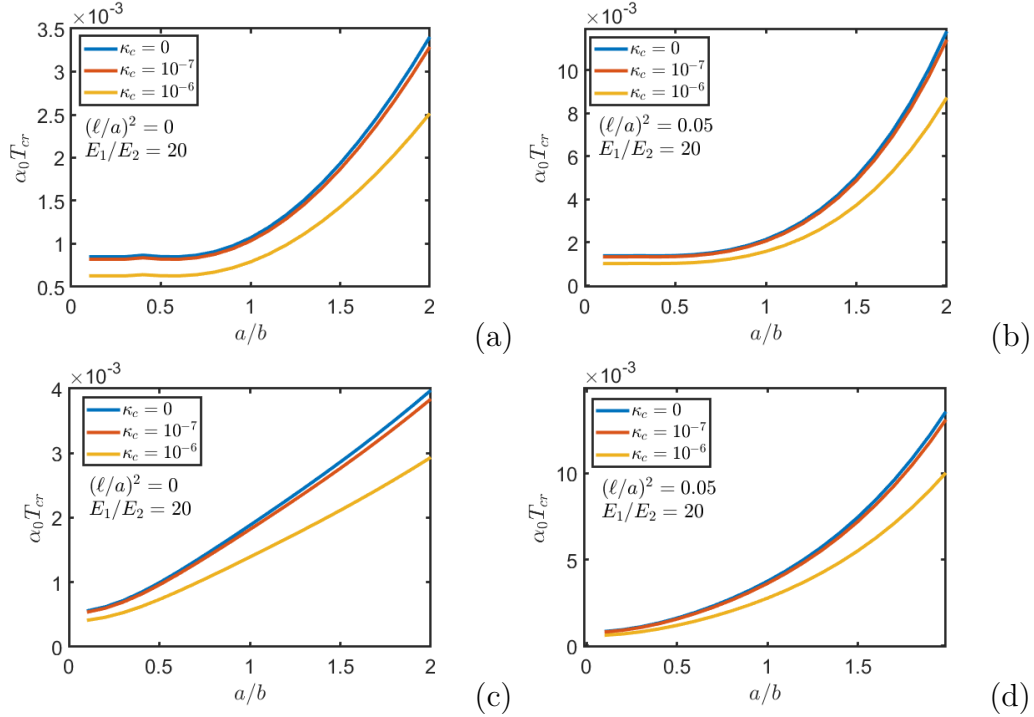


Figure 4: Critical temperature $\alpha_0 T_{cr}$ of plate by varying κ_{c_0} with lamination layout $(0/90)_2$ for $(\ell/a)^2 = 0$ (a) and for $(\ell/a)^2 = 0.05$ (b) with lamination layout $(-45/45)_2$ for $(\ell/a)^2 = 0$ (c) and for $(\ell/a)^2 = 0.05$ (d).

4.1.3. Hygrothermal loads

For hygrothermal a rectangular plate with ratio $a/b = 1.5$ with $a = 1$ is considered. Table 7 lists the combined buckling loads with $\kappa_{c_0} = C_{0,cr}/T_{0,cr}$ for both cross- and angle-ply laminates. Globally the critical temperature increases, as in the previous cases, by increasing the stiffness ratio E_1/E_2 and the nonlocal parameter. It is mentioned that by increasing the ratio $\kappa_{c_0} = C_{0,cr}/T_{0,cr}$, the critical temperature decreases because the critical load is weighted between the two values of $C_{0,cr}$ and $T_{0,cr}$. Figure 4 show the critical temperature for cross- and angle-ply laminates, when they are subjected to hygrothermal load combination. It is noted that the angle-ply laminates have a smaller exponential increase with respect to the cross-ply ones by varying the geometric ratio a/b for $a = 1$.

$(\ell/a)^2$	κ_{c_0}	E_1/E_2				
		5	10	20	25	40
$(0/90)_2$						
0.00	0	0.8432	1.2477	1.9323	2.2265	2.9657
	10^{-7}	0.8097	1.2007	1.8662	2.1538	2.8802
	10^{-6}	0.5964	0.8965	1.4271	1.6645	2.2871
0.05	0	2.1956	3.2489	5.0314	5.7975	7.7221
	10^{-7}	2.1083	3.1264	4.8594	5.6081	7.4996
	10^{-6}	1.5528	2.3343	3.7160	4.3340	5.9552
0.10	0	3.5840	5.2501	8.1304	9.3684	12.4785
	10^{-7}	3.4069	5.0521	7.8525	9.0624	12.1189
	10^{-6}	2.5093	3.7721	6.0048	7.0035	9.6233
$(-45/45)_2$						
0.00	0	1.0607	1.7302	2.8627	3.3493	4.5716
	10^{-7}	1.0185	1.6650	2.1143	3.2399	4.4398
	10^{-6}	0.7502	1.2431	2.2479	2.5038	3.5255
0.05	0	2.7618	4.5052	7.4539	8.7209	11.9035
	10^{-7}	2.6520	4.3353	7.1990	8.4360	11.5605
	10^{-6}	1.9533	3.2369	5.5051	6.5194	9.1798
0.10	0	4.4629	7.2801	12.0451	14.0925	19.2354
	10^{-7}	4.2855	7.0056	11.6333	13.6322	18.6811
	10^{-6}	3.1564	5.2307	8.8960	10.5350	14.8341

Table 7: $\alpha_0 T_{0,cr} \cdot 10^3$ of a rectangular plate ($a/b = 1.5$) with lamination layout $(0/90)_2$ for different value of ratio $\kappa_{c_0} = C_{0,cr}/T_{0,cr}$ and non local parameter $(\ell/a)^2$. $(m, n) = (1, 1)$.

212 *4.2. Free Vibration*

213 In this section results of free vibration, including thermal effects, are
214 reported. The critical temperature will be analyzed, which corresponds to
215 the temperature at which the natural frequency of free vibration becomes
216 zero. The following material properties are used in the computations below:
217 $E_1/E_2 = var.$, $\nu_{12} = 0.25$, $\nu_{13} = \nu_{23} = 0$, $G_{12} = G_{13} = 0.5E_2$, $G_{23} = 0.2E_2$,
218 $\alpha_1/\alpha_0 = 1$, $\alpha_2/\alpha_0 = 3$. The plate is considered squared $a = b = 1$ for all
219 numerical simulations. Natural frequencies are factorized as:

220 • cross-ply: $\bar{\omega} = \omega b^2/\pi^2 \sqrt{\rho h/D_{22}}$

221 • angle-ply: $\bar{\omega} = \omega a^2/h \sqrt{\rho/E_2}$

222 Table 8 lists the results compared to [48, 52]. The results of the present work
223 agree well with the ones presented in former literature but these results do
224 not include any hygrothermal effect.

225 Figure 5 shows the influence of temperature in natural vibration frequen-
226 cies of cross- and angle-ply laminates for different values of non local pa-
227 rameter and different lamination layouts. By reducing the temperature a
228 detrimental effect is observed in the structural stiffness since the main nat-
229 ural frequency reduces garishly. There exists a temperature value for which
230 the natural frequency is equal to zero, that temperature is called critical
231 temperature for free vibrations. It can be noted that critical temperature
232 for angle-ply laminates is higher than those of cross-ply laminates for plates
233 with same number of laminae. In other words angle-ply laminates are able
234 to vibrate at higher temperatures with respect to cross-ply before collapse.
235 The same evidence is reported in tabular form in table 9 where critical tem-
236 peratures for cross- and angle-ply laminates are provided.

237 **5. Conclusions**

238 In this paper, hygrothermal buckling and dynamic problems of simply
239 supported composite nano plates were investigated. Non local second strain
240 gradient theory is implemented for taking into account the effects of nano
241 scale. Through Hamilton's principle motion equations for laminated com-
242 posite thin plates are derived. The analytical solution using Navier solution
243 method is obtained. Several plate layouts, materials and geometries are
244 involved, comparisons for the classical case wherever it was possible are pro-
245 vided, then outcomes are extended to non local theory. Firstly outcomes for

Layout	$(\ell/a)^2$	Ref. [48]	Ref. [52]	Present
$E_1/E_2 = 10$				
(0/90)	0	1.183	1.183	1.183
	0.05	—	1.668	1.668
	0.10	—	2.041	2.040
(0/90) ₄	0	1.545	1.545	1.545
	0.05	—	2.178	2.177
	0.10	—	2.664	2.664
$E_1/E_2 = 20$				
(0/90)	0	0.990	0.990	0.990
	0.05	—	1.395	1.395
	0.10	—	1.707	1.707
(0/90) ₄	0	1.469	1.469	1.469
	0.05	—	2.071	2.071
	0.10	—	2.534	2.534
$E_1/E_2 = 25$				
(−45/45)	0	12.357	12.358	12.357
	0.05	—	17.419	17.419
	0.10	—	21.311	21.310
(−45/45) ₄	0	20.154	20.154	20.154
	0.05	—	28.409	28.409
	0.10	—	34.756	34.756
$E_1/E_2 = 40$				
(−45/45)	0	14.636	14.636	14.636
	0.05	—	20.631	20.630
	0.10	—	25.241	25.239
(−45/45) ₃	0	24.825	24.825	24.825
	0.05	—	34.994	34.994
	0.10	—	42.812	42.811

Table 8: Fundamental frequencies $\bar{\omega}$ for cross- and angle-ply laminates.

$(\ell/a)^2$	(0/90)	(0/90) ₄	(−45/45)	(−45/45) ₄
0	35.2506	77.6826	55.5655	138.4088
0.05	70.0422	154.3526	110.4064	275.0129
0.10	104.8334	231.0231	165.2473	411.6170

Table 9: Critical temperature $T_{0,cr}$ for cross- and angle-ply laminates with $E_1/E_2 = 20$.

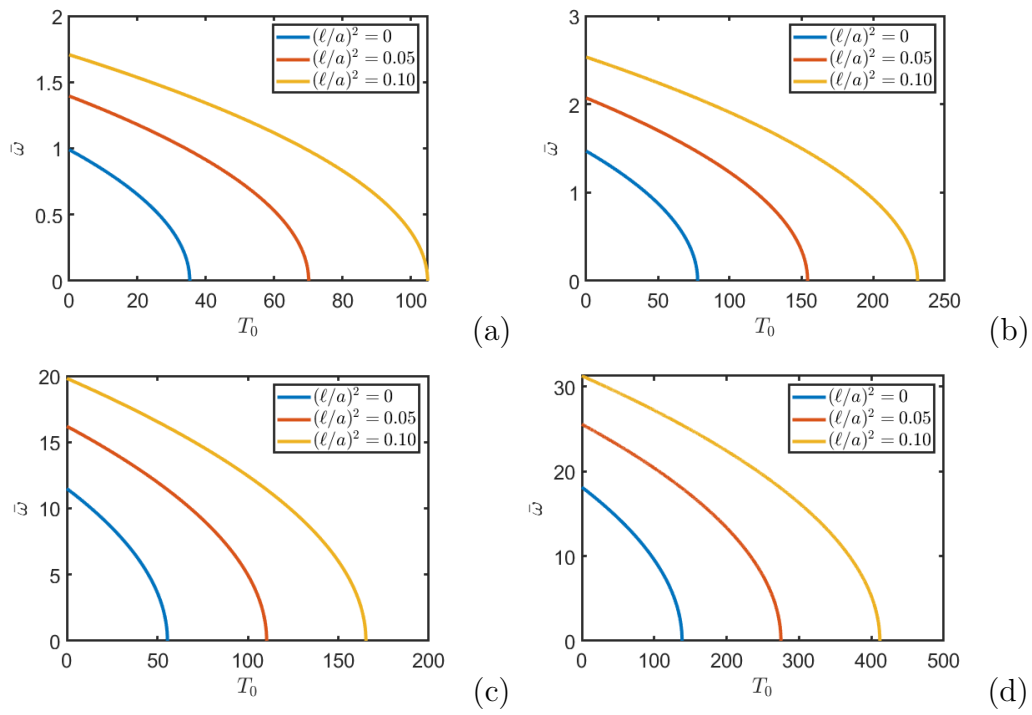


Figure 5: Natural frequency ($\bar{\omega}$) versus temperature (T_0) with $E_1/E_2 = 20$ for (a) $(0/90)$, (b) $(0/90)_4$, (c) $(-45/45)$ and (d) $(-45/45)_4$.

246 thermal and combined hygrothermal buckling of cross- and angle-ply lam-
247 inates are provided, it can be seen that for the same number of laminae,
248 angle-ply laminates are preferable, moreover for the same thickness is better
249 to have more laminae. Finally outcomes for free vibration are reported. At
250 first the classic problem is investigated and compared, then thermal terms
251 are included and the critical temperatures for various lamination layouts and
252 values of non local parameter is obtained. Also in this case, angle-ply lami-
253 nates show a better behavior than cross-ply ones.

254 **References**

- 255 [1] V. S. Saji, H. C. Choe, K. W. Yeung, Nanotechnology in biomedical
256 applications: a review, *International Journal of Nano and Biomaterials*
257 3 (2010) 119–139.
- 258 [2] D. Berman, J. Krim, Surface science, MEMS and NEMS: Progress and
259 opportunities for surface science research performed on, or by, microde-
260 vices, *Progress in Surface Science* 88 (2013) 171 – 211.
- 261 [3] B. Bhushan, Nanotribology and nanomechanics of MEMS/NEMS and
262 bioMEMS/bioNEMS materials and devices, *Microelectronic Engineer-*
263 *ing* 84 (2007) 387 – 412. Nanoscale imaging and metrology of devices
264 and innovative materials.
- 265 [4] K. L. Ekinici, M. L. Roukes, Nanoelectromechanical systems, *Review of*
266 *Scientific Instruments* 76 (2005) 061101.
- 267 [5] A. Bonanni, M. del Valle, Use of nanomaterials for impedimetric DNA
268 sensors: A review, *Analytica Chimica Acta* 678 (2010) 7 – 17.
- 269 [6] W. Wu, Inorganic nanomaterials for printed electronics: a review,
270 *Nanoscale* 9 (2017) 7342–7372.
- 271 [7] O. Gohardani, M. C. Elola, C. Elizetxea, Potential and prospective im-
272 plementation of carbon nanotubes on next generation aircraft and space
273 vehicles: A review of current and expected applications in aerospace
274 sciences, *Progress in Aerospace Sciences* 70 (2014) 42 – 68.
- 275 [8] T. Singh, A review of nanomaterials in civil engineering works, *Inter J*
276 *Struct Civ Eng Res* 3 (2014) 31–5.

- 277 [9] A. W. McFarland, J. S. Colton, Role of material microstructure in plate
278 stiffness with relevance to microcantilever sensors, *Journal of Microme-*
279 *chanics and Microengineering* 15 (2005) 1060–1067.
- 280 [10] D. Lam, F. Yang, A. Chong, J. Wang, P. Tong, Experiments and theory
281 in strain gradient elasticity, *Journal of the Mechanics and Physics of*
282 *Solids* 51 (2003) 1477 – 1508.
- 283 [11] R. Lakes, Experimental microelasticity of two porous solids, *Internation-*
284 *al Journal of Solids and Structures* 22 (1986) 55 – 63.
- 285 [12] J. Stölken, A. Evans, A microbend test method for measuring the plas-
286 ticity length scale, *Acta Materialia* 46 (1998) 5109 – 5115.
- 287 [13] A. Eringen, D. Edelen, On nonlocal elasticity, *International Journal of*
288 *Engineering Science* 10 (1972) 233 – 248.
- 289 [14] P. Trovalusci, *Molecular Approaches for Multifield Continua: origins*
290 *and current developments*, 2014, pp. 211–278.
- 291 [15] A. C. Eringen, On differential equations of nonlocal elasticity and solu-
292 tions of screw dislocation and surface waves, *Journal of Applied Physics*
293 54 (1983) 4703–4710.
- 294 [16] E. Aifantis, Update on a class of gradient theories, *Mechanics of Mate-*
295 *rials* 35 (2003) 259 – 280.
- 296 [17] J. Meenen, H. Altenbach, V. Eremeyev, K. Naumenko, A variationally
297 consistent derivation of microcontinuum theories, *Advanced Structured*
298 *Materials* 15 (2011).
- 299 [18] R. Mindlin, N. Eshel, On first strain-gradient theories in linear elasticity,
300 *International Journal of Solids and Structures* 4 (1968) 109 – 124.
- 301 [19] B. Karami, M. Janghorban, T. Rabczuk, Static analysis of function-
302 ally graded anisotropic nanoplates using nonlocal strain gradient theory,
303 *Composite Structures* 227 (2019) 111249.
- 304 [20] V. Eremeyev, H. Altenbach, On the Direct Approach in the Theory of
305 *Second Gradient Plates*, volume 45, 2015, pp. 147–154.

- 306 [21] M. Baccocchi, N. Fantuzzi, A. Ferreira, Conforming and nonconforming
307 laminated finite element Kirchhoff nanoplates in bending using strain
308 gradient theory, *Computers & Structures* 239 (2020) 106322.
- 309 [22] R. Barretta, L. Feo, R. Luciano, F. Marotti de Sciarra, R. Penna, Func-
310 tionally graded Timoshenko nanobeams: A novel nonlocal gradient for-
311 mulation, *Composites Part B: Engineering* 100 (2016) 208 – 219.
- 312 [23] S. Sahmani, M. M. Aghdam, T. Rabczuk, Nonlinear bending of function-
313 ally graded porous micro/nano-beams reinforced with graphene platelets
314 based upon nonlocal strain gradient theory, *Composite Structures* 186
315 (2018) 68 – 78.
- 316 [24] A. Jamalpoor, M. Hosseini, Biaxial buckling analysis of double-
317 orthotropic microplate-systems including in-plane magnetic field based
318 on strain gradient theory, *Composites Part B: Engineering* 75 (2015) 53
319 – 64.
- 320 [25] A. Apuzzo, R. Barretta, S. Faghidian, R. Luciano, F. Marotti de Sciarra,
321 Free vibrations of elastic beams by modified nonlocal strain gradient
322 theory, *International Journal of Engineering Science* 133 (2018) 99 –
323 108.
- 324 [26] F. Yang, A. Chong, D. Lam, P. Tong, Couple stress based strain gradient
325 theory for elasticity, *International Journal of Solids and Structures* 39
326 (2002) 2731 – 2743.
- 327 [27] H. Mühlhaus, F. Oka, Dispersion and wave propagation in discrete and
328 continuous models for granular materials, *International Journal of Solids
329 and Structures* 33 (1996) 2841 – 2858.
- 330 [28] L. Leonetti, F. Greco, P. Trovalusci, R. Luciano, R. Masiani, A
331 multiscale damage analysis of periodic composites using a couple-
332 stress/Cauchy multidomain model: Application to masonry structures,
333 *Composites Part B: Engineering* 141 (2018) 50 – 59.
- 334 [29] A. Farajpour, C. Q. Howard, W. S. Robertson, On size-dependent me-
335 chanics of nanoplates, *International Journal of Engineering Science* 156
336 (2020) 103368.

- 337 [30] R. Barretta, S. A. Faghidian, F. Marotti de Sciarra, Stress-driven nonlo-
338 cal integral elasticity for axisymmetric nano-plates, *International Jour-*
339 *nal of Engineering Science* 136 (2019) 38 – 52.
- 340 [31] P. Trovalusci, M. D. Bellis, M. Ostoja-Starzewski, A statistically-based
341 homogenization approach for particle random composites as micropolar
342 continua., *Advanced Structured Materials* 42 (2016).
- 343 [32] E. Reccia, M. L. De Bellis, P. Trovalusci, R. Masiani, Sensitivity to
344 material contrast in homogenization of random particle composites as
345 micropolar continua, *Composites Part B: Engineering* 136 (2018) 39 –
346 45.
- 347 [33] N. Fantuzzi, L. Leonetti, P. Trovalusci, F. Tornabene, Some novel nu-
348 merical applications of Cosserat continua, *International Journal of Com-*
349 *putational Methods* 15 (2018) 1850054.
- 350 [34] F. Pinnola, S. A. Faghidian, R. Barretta, F. Marotti de Sciarra, Varia-
351 tionally consistent dynamics of nonlocal gradient elastic beams, *Inter-*
352 *national Journal of Engineering Science* 149 (2020) 103220.
- 353 [35] M. Mohammadimehr, M. Salemi, B. Roustana Navi, Bending, buckling,
354 and free vibration analysis of MSGT microcomposite Reddy plate rein-
355 forced by FG-SWCNTs with temperature-dependent material properties
356 under hydro-thermo-mechanical loadings using DQM, *Composite Struc-*
357 *tures* 138 (2016) 361 – 380.
- 358 [36] M. Arefi, A. M. Zenkour, Thermo-electro-mechanical bending behavior
359 of sandwich nanoplate integrated with piezoelectric face-sheets based on
360 trigonometric plate theory, *Composite Structures* 162 (2017) 108 – 122.
- 361 [37] J. Yan, L. Tong, C. Li, Y. Zhu, Z. Wang, Exact solutions of bending
362 deflections for nano-beams and nano-plates based on nonlocal elasticity
363 theory, *Composite Structures* 125 (2015) 304 – 313.
- 364 [38] C. H. Thai, A. Ferreira, P. Phung-Van, A nonlocal strain gradient iso-
365 geometric model for free vibration and bending analyses of functionally
366 graded plates, *Composite Structures* 251 (2020) 112634.

- 367 [39] L. Lu, X. Guo, J. Zhao, Size-dependent vibration analysis of nanobeams
368 based on the nonlocal strain gradient theory, *International Journal of*
369 *Engineering Science* 116 (2017) 12 – 24.
- 370 [40] H. Daghigh, V. Daghigh, A. Milani, D. Tannant, T. E. Lacy, J. Reddy,
371 Nonlocal bending and buckling of agglomerated cnt-reinforced compos-
372 ite nanoplates, *Composites Part B: Engineering* 183 (2020) 107716.
- 373 [41] A. Jafari, S. Shirvani Shah-enayati, A. A. Atai, Size dependency in
374 vibration analysis of nano plates; one problem, different answers, *Euro-*
375 *pean Journal of Mechanics - A/Solids* 59 (2016) 124 – 139.
- 376 [42] O. Civalek, C. Demir, B. Akgoz, Free vibration and bending analyses
377 of cantilever microtubules based on nonlocal continuum model, *Mathe-*
378 *matical and Computational Applications* 15 (2010) 289 – 298.
- 379 [43] L. Chu, G. Dui, Y. Zheng, Thermally induced nonlinear dynamic
380 analysis of temperature-dependent functionally graded flexoelectric
381 nanobeams based on nonlocal simplified strain gradient elasticity theory,
382 *European Journal of Mechanics - A/Solids* 82 (2020) 103999.
- 383 [44] S. Brischetto, R. Leetsch, E. Carrera, T. Wallmersperger, B. Kröplin,
384 Thermo-mechanical bending of functionally graded plates, *Journal of*
385 *Thermal Stresses* 31 (2008) 286–308.
- 386 [45] S. Brischetto, Hygrothermal loading effects in bending analysis of multi-
387 layered composite plates, *Computer Modeling in Engineering & Sciences*
388 88 (2012) 367–418.
- 389 [46] S. Brischetto, E. Carrera, Coupled thermo-electro-mechanical analysis
390 of smart plates embedding composite and piezoelectric layers, *Journal*
391 *of Thermal Stresses* 35 (2012) 766–804.
- 392 [47] S. Brischetto, E. Carrera, Static analysis of multilayered smart shells
393 subjected to mechanical, thermal and electrical loads, *Meccanica* 48
394 (2013) 1263–1287.
- 395 [48] J. Reddy, *Mechanics of Laminated Composite Plates and Shells: Theory*
396 *and Analysis*, Second Edition, CRC Press, 2003.

- 397 [49] F. Cornacchia, N. Fantuzzi, R. Luciano, R. Penna, Solution for cross-
398 and angle-ply laminated Kirchhoff nano plates in bending using strain
399 gradient theory, *Composites Part B: Engineering* 173 (2019) 107006.
- 400 [50] H. Matsunaga, Thermal buckling of cross-ply laminated composite and
401 sandwich plates according to a global higher-order deformation theory,
402 *Composite Structures* 68 (2005) 439 – 454.
- 403 [51] C. M. Yucheng Shi, Raymond Y. Y. Lee, Thermal postbuckling of com-
404 posite plates using the finite element model coordinate method, *Journal*
405 *of Thermal Stresses* 22 (1999) 595–614.
- 406 [52] F. Cornacchia, F. Fabbrocino, N. Fantuzzi, R. Luciano, R. Penna, Ana-
407 lytical solution of cross- and angle-ply nano plates with strain gradient
408 theory for linear vibrations and buckling, *Mechanics of Advanced Ma-*
409 *terials and Structures* (2019).